

Supporting Information for

Similarity of Multicomponent Nanomaterials in a Safer-by-Design context: the case of Core-shell Quantum Dots

Veronica Di Battista^{a,b*}, Karla R. Sanchez-Lievanos^{a,c*}, Nina Jeliaskova^d, Fiona Murphy^e, Georgia Tsiliki^{f,g}, Alex Zabeo^h, Agnieszka Gajewicz-Skretnaⁱ, Alicja Mikołajczyk^{i,j}, Danail Hristozov^k, Vicki Stone^e, Otmar Schmid^l, Neil Hunt^m, Agnes G. Oomen^{n,o}, Wendel Wohlleben^a

^aDepartment of Analytical and Material Science and Department of Experimental Toxicology and Ecology, BASF SE, Ludwigshafen, Germany

^bDTU, Department of Environmental and Resource Engineering, Kgs. Lyngby, Denmark.

^cDepartment of Chemistry, University of Rochester, Rochester, New York 14627, United States

^dIdeaconsult Ltd., 4 Angel Kanchev St, 1000 Sofia, Bulgaria

^eHeriot-Watt-University, Edinburgh, UK

^fAthena Research Center, AthensArtemidos 6 & Epidavrou, 15125, Marousi, Greece,

^gPurposeful IKE, 144 Triths Septemvriou, 11251, Athens, Greece

^hGreenDecision, Venice, Italy

ⁱLaboratory of Environmental Chemoinformatics, Faculty of Chemistry, University of Gdansk (UG), Gdansk, Poland

^jQSAR Lab Sp. Z o. o., Trzy Lipy 3, 80-172, Poland

^kEmerge, Sofia, Bulgaria

^lInstitute of Lung Health and Immunity, Helmholtz Center Munich – German Center for Environmental Health, 85764 Neuherberg/Munich, Germany

^mThe REACH center Lancaster

ⁿNational Institute for Public Health and the Environment (RIVM), Bilthoven, the Netherlands

^oInstitute for Biodiversity and Ecosystem Dynamics, University of Amsterdam (UvA), the Netherlands

Contents

Figure S1. Dissolution setup.	2
Figure S2. Time-resolved dissolution kinetics of QDs in pH7.4 Gamble's or "LSF" medium.	3
Figure S3. Fluorescence emission spectra of ZnCuInS, ZnCuInS-COOH-L and ZnCdSeS in water.	3
Figure S4.(A) Comparison between the two descriptors Dissolved ion % and leachable mass % in PSF, obtained from one week abiotic dissolution, for all metallic elements from the 5 QDs. ZnO and CuO materials are included for benchmarking. (B)Schematic representation of the two descriptors reported in (A). Changes in %wt are reported and shown to be minimal. Grey dots represent the remaining %wt of each QDs constituted by polymer. All dissolution experiments were done in duplicates with an average standard deviation at each sampling point of 1-3%.	4
Figure S5. Flow diagram showing the relevant questions to be answered for predicting hazard endpoints in physiological media, here addressed using Tier 1 in chemico data and considered for similarity assessment and grouping analysis.	5
Figure S6. Representative TEM micrographs of the 5 QDs under study prior and after incubation for 168 h in PSF. The scale bar represents 10 nm.	6
Figure S7. WOWA approach similarity analysis with respect to Mass specific surface area and diameter.	7
Table S2. Composition of phagolysosomal (PSF) and lung simulant fluids (LSF) (in g) for 5L of Nanopure H ₂ O at 37°C.	9

Table S3. Examples of international occupational exposure limits in air for some elements of concern in commercially available QDs. These OELs are set by regulatory authorities considering the available data on carcinogenicity, mutagenicity and toxicity to reproduction.	9
Table S4. Properties derived from the present study and main categorization outcomes for the QDs family	10

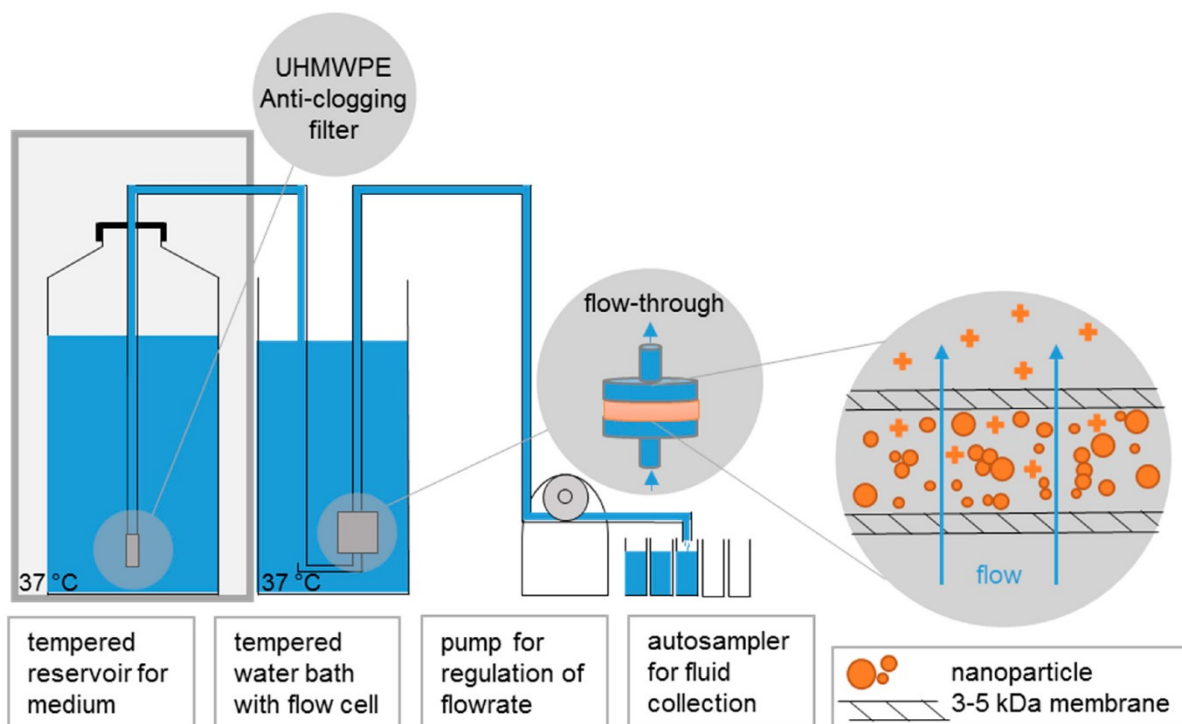


Figure S1. Dissolution setup. Reproduced with permission of reference ¹.

We investigate the dissolution kinetics of QDs under the PSF environment previously developed by NIOSH because the acidic lysosomal condition (pH4.5) can be used to best predict the biodissolution behavior of inhaled nanomaterials. Additionally, we use the recommended ISO standard (ISO/TR19057, 2017) for non-lysosomal conditions as a complementary medium that mimics the pH 7.4 condition of extracellular lung fluid. This fluid contains strong metal-ion chelator citrate ligands to mimic the organic constituents (lipids, proteins) of the natural fluids (Table S1). We acknowledge that for some metal-based nanomaterials, this medium may exaggerate their potential to dissolve and transform, but since cellular uptake and subsequent lysosomal dissolution is considered one of the main pathways of metal-induced toxicity, the structural transformation should be maximized for our methodical purpose to evaluate transformation as potential criteria for hazard grouping.

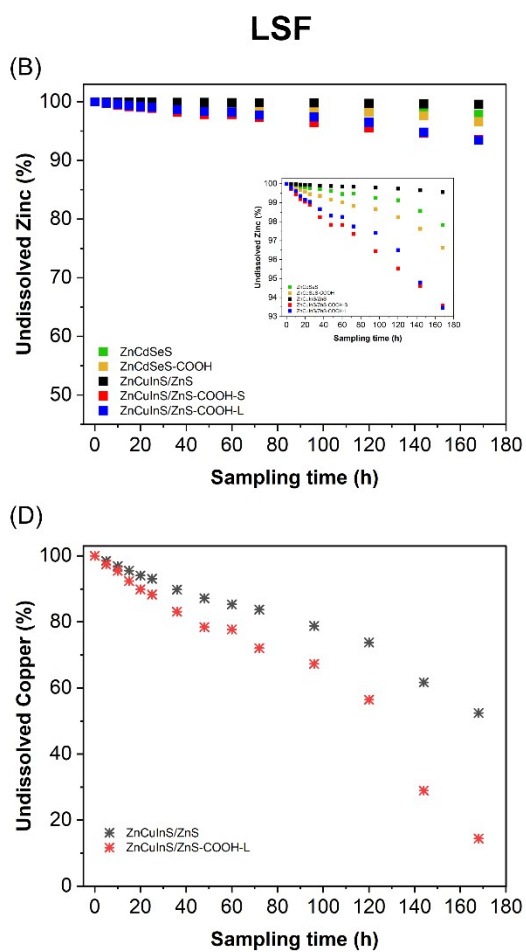


Figure S2. Time-resolved dissolution kinetics of QDs in pH7.4 Gamble's or "LSF" medium.

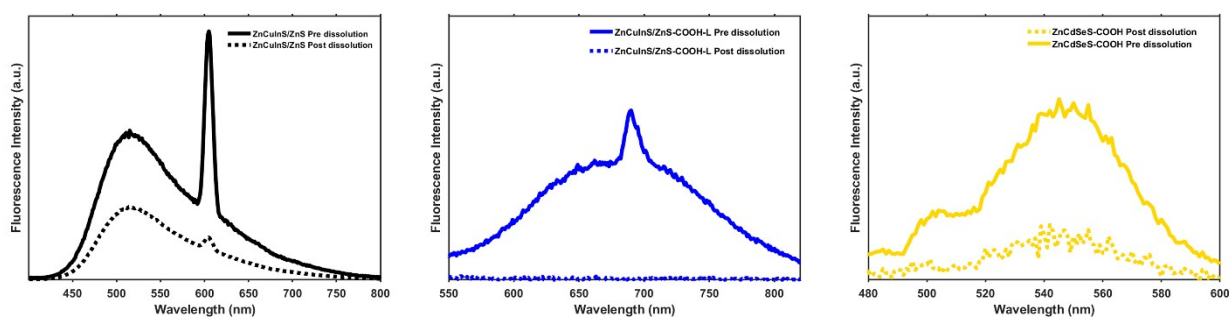


Figure S3. Fluorescence emission spectra of ZnCuInS, ZnCuInS-COOH-L and ZnCdSeS in water.

(A)

Dissolved ion%: % of the single metal component which turns into ions	%Zn	%Cd	%Se	%Cu	%In
ZnCuInS/ZnS	2.3			41.5	0.2
ZnCuInS/ZnS-COOH-S	27.9			86.3	3.9
ZnCuInS/ZnS-COOH-L	51.4			42.1	7.2
ZnCdSeS	3.9	0.004	<LOD		
ZnCdSeS-COOH	1.3	0.1	<LOD		
ZnO	88.1				
CuO				96.3	
Leachable mass%: % out of the initial loaded mass that turns into ions	%Zn	%Cd	%Se	%Cu	%In
ZnCuInS/ZnS	0.4			0.1	0.02
ZnCuInS/ZnS-COOH-S	0.4			0.02	0.01
ZnCuInS/ZnS-COOH-L	0.8			0.08	0.03
ZnCdSeS	1.3	0.00042	<LOD		
ZnCdSeS-COOH	0.4	0.02	<LOD		
ZnO	70.4				
CuO				77.1	

(B)

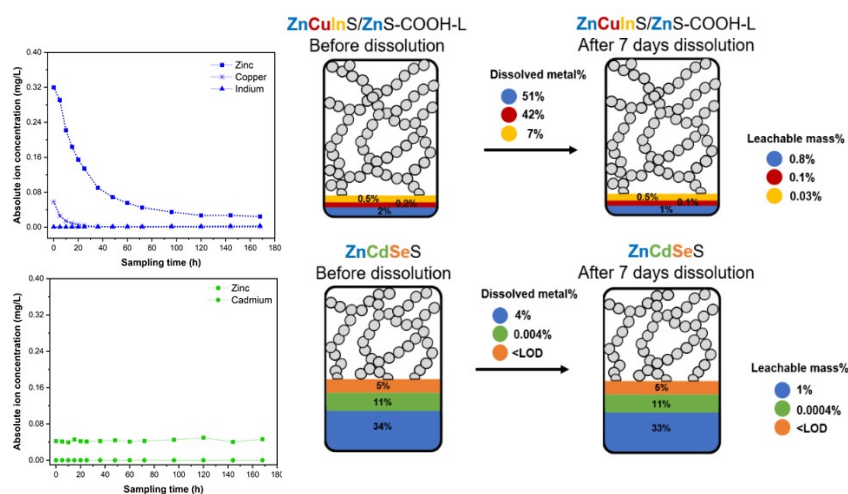


Figure S4. (A) Comparison between the two descriptors Dissolved ion % and leachable mass % in PSF, obtained from one week abiotic dissolution, for all metallic elements from the 5 QDs. ZnO and CuO materials are included for benchmarking. (B) Schematic representation of the two descriptors reported in (A). Changes in %wt are reported and shown to be minimal. Grey dots represent the remaining %wt of each QDs constituted by polymer. All dissolution experiments were done in duplicates with an average standard deviation at each sampling point of 1-3%.

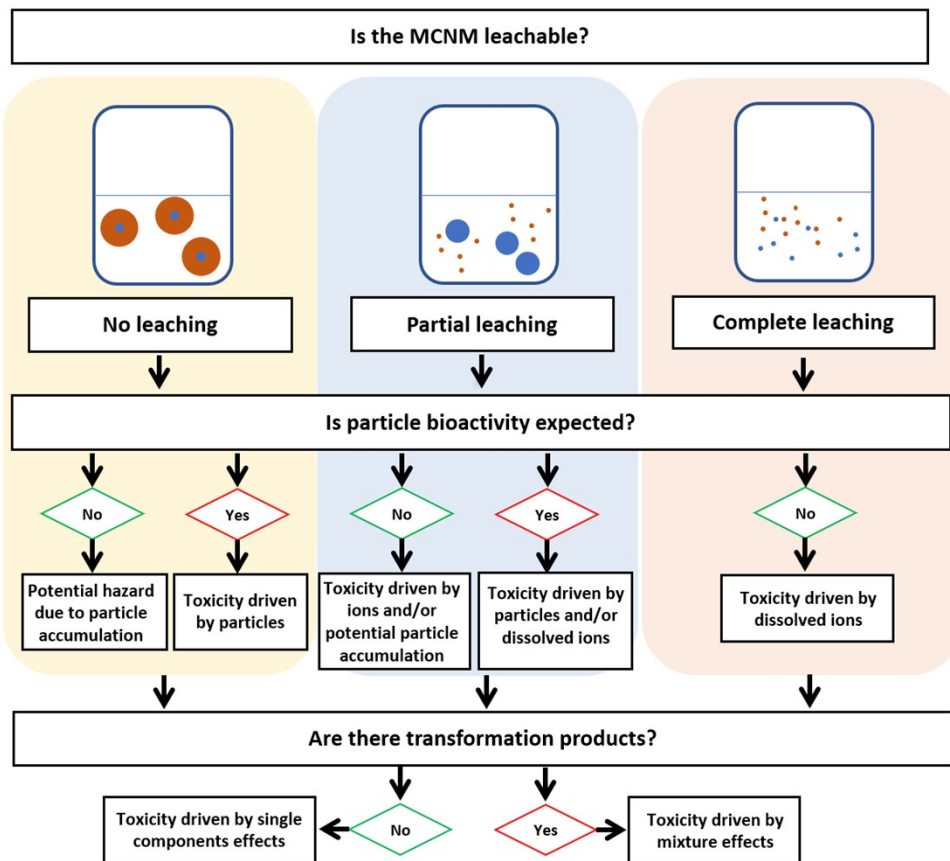


Figure S5. Flow diagram showing the relevant questions to be answered for predicting hazard endpoints in physiological media, here addressed using Tier 1 in chemico data and considered for similarity assessment and grouping analysis.

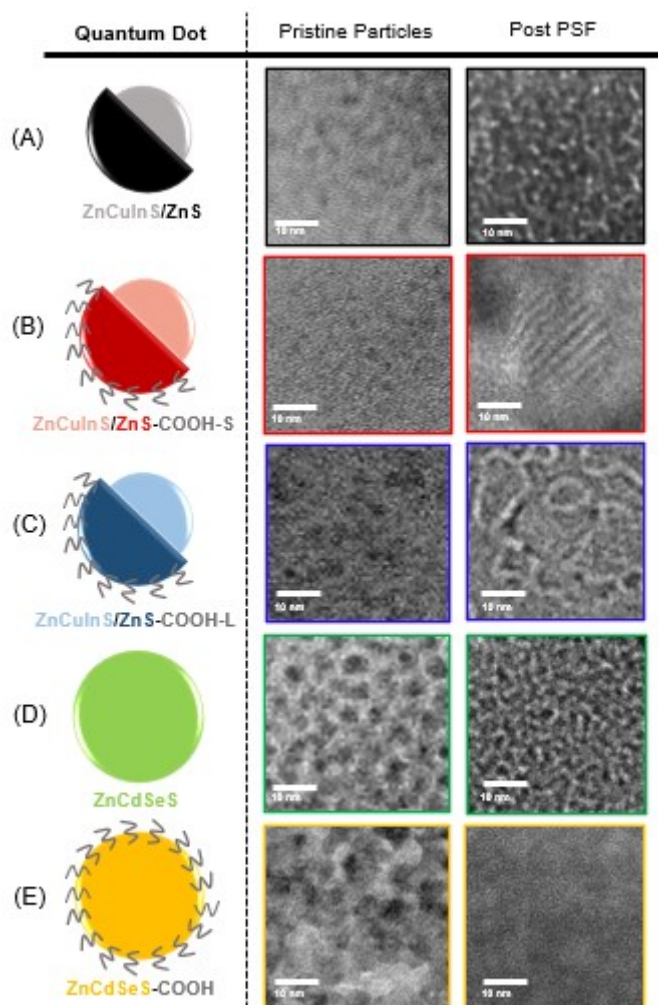


Figure S6. Representative TEM micrographs of the 5 QDs under study prior and after incubation for 168 h in PSF. The scale bar represents 10 nm.

Figure S6 showcases the fluorescence emission spectra of the other three QDs, where ZnCuInS/ZnS retains its optical properties, ZnCuInS/ZnS-COOH-L shows no substantial trace of PL, and ZnCdSeS-COOH, because of low recovered amounts, presents a discernable low signal-to-noise ratio emission spectrum. We investigated the transformation of structural details after abiotic testing. Figure S6 contains representative TEM micrographs of both pristine and post-dissolution (in PSF) QDs. We found traces of QDs only in the ZnCuInS/ZnS and ZnCdSeS cases. The other samples contained mostly Zn and S as trace elements. All the TEM grids with post-dissolution hydrophilic QDs contained other elemental traces (Na, Ca, K, Mg, and Cl) from the PSF medium. After performing EDXS on the post-dissolution ZnCuInS/ZnS QD, no copper traces could be found, which agrees with the results from the dissolution experiment, where up to 42% of the copper ion content within the sample had leached. The initial content of copper was initially significantly low (0.31%wt), confirming that its substantial leaching led to its barely detectable amount. Figure S6B displays a shift towards larger crystallite diameters on post-dissolution ZnCuInS/ZnS-COOH-S QDs. This observation can be explained by assuming the Ostwald ripening model, in which the minimization of interfacial energy is achieved by the dissolution of small crystals and - mediated by the minimal ion's solubility

- subsequent redeposition of the dissolved species on the surfaces of larger crystals. Despite finding traces of all the elemental components, the TEM micrograph scope area in Fig. S6B, did not show any photoluminescence at all, which can be associated with the resulting enlarged crystallites that deviate from the quantum confinement size regime. Figures S6C and S6E post-dissolution micrographs show amorphous deposited material with lower content of all the elements of interest within ZnCuInS-COOH-L and ZnCdSeS-COOH (EDX prior-/after dissolution), suggesting partial dissolution of QDs. The lack of crystalline structure is associated with the observed loss of photoluminescence.



Figure S7. WOWA approach similarity analysis with respect to Mass specific surface area and diameter.

Table S1. Overview of QDs physicochemical properties. The size of QDs was calculated based on one representative TEM image including 200-300 particles. Values were confirmed with those reported on www.plasmachem.com. The Surface area was calculated from the particle size and the respective density available on the producer website. (www.plasmachem.com)

Code name	Reference number ^a	Minimum external dimension (nm) ^b	Shape ^a	Elemental composition (%wt) ^c	Mass-specific Surface Area from TEM (m ² /g)	Surface chemistry ^d
ZnCuInS/ZnS	PL-QD-CF-530-100mg	3.3	Isotropic spheres	Zn:19.2 Cu:0.31 In:9.03	255	O: 3.78 ±0.43, C: 93.92 ±0.44, N: 2.30 ±0.20
ZnCuInS/ZnS-COOH-S	PL-QD-WCF-530-100mg	3.4	Isotropic spheres	Zn:1.46 Cu:0.02 In:0.34	247	B: 7.90 ±3.39, O: 27.97±3.08, C: 53.53±8.75, Na: 8.06 ±1.66, Cl: 1.37 ±1.19
ZnCuInS/ZnS-COOH-L	PL-QD-WCF-700-100mg	4.6	Isotropic spheres	Zn:1.58 Cu:0.21 In:0.46	183	B: 3.12 ±1.64, O: 19.52± 1.67, C: 70.64 ±3.29, Na: 6.05 ±0.10, Cl: 0.37 ±0.36
ZnCdSeS	PL-QD-OA-530-100mg	5.7	Isotropic spheres	Zn:33.87 Cd:10.58 Se:5.69	147	C: 63.83 ±2.25, O: 9.41 ±1.63, Zn: 12.95 ±0.37, Cd: 0.76± 0.06, Se: 0.79± 0.26, S: 12.26 ±1.45 Likely overestimated because of Se 3p-S2p overlapping.
ZnCdSeS-COOH	PL-QD-WA-530-100mg	5.2	Isotropic spheres	Zn:32.73 Cd:20.47 Se:7.09	162	B: 11.19 ± 1.85, O: 40.48 ±1.92, C: 35.20 ±4.13, Na: 11.12 ±0.80, Cl: 2.02 ±0.21

^aPlasmaChem

^bExperimentally characterized by TEM

^cExperimentally characterized by ICPMS

^dExperimentally characterized by XPS

Table S2. Composition of phagolysosomal (PSF) and lung simulant fluids (LSF) (in g) for 5L of Nanopure H₂O at 37°C

<i>Substance</i>	<i>PSF</i>	<i>LSF</i>
Na ₂ HPO ₄	0.710	
NaHPO ₄		0.630
NaCl	33.250	30.095
Na ₂ SO ₄	0.355	0.315
CaCl ₂ · 2H ₂ O	0.145	1.840
Glycine	2.250	
KH-Phthalate	20.423	
Alkylbenzyltrimethylammonium chloride (ABDC)	0.250	
NaN ₃	0.100	0.100
MgCl ₂ · 6H ₂ O		0.924
KCl		1.490
NaHPO ₄		0.630
Sodium acetate		2.870
NaHCO ₃		13.020
Na ₃ Citrate · 2H ₂ O		0.485

Table S3. Examples of international occupational exposure limits in air for some elements of concern in commercially available QDs. These OELs are set by regulatory authorities considering the available data on carcinogenicity, mutagenicity and toxicity to reproduction.

Element	Regulation Dossier Limit / OEL (mg/m ³)
Cu	1 ^a
Zn	5 ^b
In	0.1 ^c
Cd	1.8x10 ⁻⁶ ^d

^aWHO/OSHA^bREACH/ECHA^c REACH/ECHA^dUS EPA

Table S4. Properties derived from the present study and main categorization outcomes for the QDs family

QDot	Leaching	MAK scaled leaching	Particles Reactivity	Ions reactivity	Transformation product	Hypothesis
ZnCuInS/ZnS	Partial leaching	Low	Low particles reactivity at 1 g/L	Yes	No. Retains optical properties.	Potential hazard due to particle accumulation and dissolved ions
ZnCuInS/ZnS-COOH_S	Partial leaching	Low	Low particles reactivity at 1 g/L	Yes	Yes. No trace of optical properties	Potential hazard due to particles accumulation and mixture effects
ZnCuInS/ZnS-COOH_L	Partial leaching	Low	Low particles reactivity at 1 g/L	Yes	Yes. No trace of optical properties	Potential hazard due to particle accumulation, dissolved ions and mixture effects
ZnCdSeS	Partial leaching	High Presence of Cd	High particles reactivity at 1 g/L	No	No. Retains optical properties.	Toxicity driven by particles
ZnCdSeS-COOH	Partial leaching	High Presence of Cd	Low particles reactivity at 1 g/L	No	No. Retains optical properties.	Potential hazard due to particle accumulation

References

- (1) Keller, J. G.; Peijnenburg, W.; Werle, K.; Landsiedel, R.; Wohlleben, W. Understanding Dissolution Rates via Continuous Flow Systems with Physiologically Relevant Metal Ion Saturation in Lysosome. *Nanomaterials* **2020**, *10* (2), 311.